Supporting Information

Locating the Reaction Site of 1,2,3,4-Butanetetracarboxylic Acid Carboxyl and Cellulose Hydroxyl in the Esterification Cross-Linking

Bolin Ji[a,d,e], Xiaowen Wang[a], Shoujia Gong[a], Weibing Zhong[b], and Ruyi Xie[c,d*]

[a]*National Engineering Research Center for Dyeing and Finishing of Textiles, College of Chemistry, Chemical Engineering and Biotechnology, Donghua University, Shanghai 201620, PR China*

[b]*State Key Laboratory of New Textile Materials and Advanced Processing Technologies, Wuhan Textile University, Wuhan 430200, PR China*

[c]*College of Textiles & Clothing, Qingdao University, Qingdao 266071, PR China*

[d]*National Innovation Center of Advanced Dyeing and Finishing Technology, Tai'an, 271000, PR China*

[e]*State Key Laboratory of Bio-Fibers and Eco-Textiles, Qingdao University, Qingdao 266071, PR China*

*Corresponding author: Email: xieruyi@qdu.edu.cn,

Address: Qingdao University, No. 308, Ningxia Road, Shinan District, Qingdao 266071, PR China.

Figure S1. FTIR spectra of BTCA and cellobiose mixture at different temperatures.

Table S1. Tentative assignments of absorbance of cellulose fabric and BTCA.

Table S2. The sign of cross peaks between 3660 and 3050 cm^{-1} in 2Dcos maps and their changing order.

Table S3. The sign of cross peaks between 1812 and 1591 cm^{-1} in 2Dcos maps and their changing order.
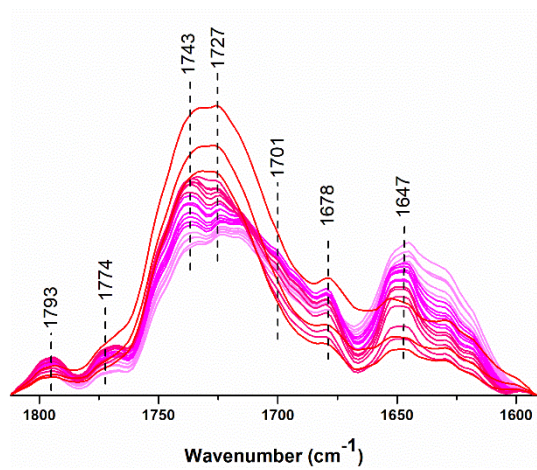
Figure S1. FTIR spectra of BTCA and cellobiose mixture at different temperatures.

Table S1. Tentative assignment of absorbance of cellulose fabric and BTCA.[1-5]

Wavenumber (cm^{-1})	Tentative assignments
3574	v(O–H) (cellulose, free)
3441	v(O(2)–H(2)$\cdots$O(6)) (cellulose, intrachain)
3410	v(O(6)–H(6)$\cdots$O(3)) (cellulose, interchain)
3334	v(O(3)–H(3)$\cdots$O(5)) (cellulose, intrachain)
3220	v(O–H) (cellulose, weak hydrogen-bonded)
1777	v(C=O) (BTCA, anhydride)
1704	v(C=O) (BTCA carboxyl carbonyl, weak hydrogen-bonded; or ester carboxyl carbonyl)
1697	v(C=O) (BTCA carboxyl carbonyl, hydrogen-bonded)
1647	v(C–O) (water)
1435	δ(C(6)–H(6)) (cellulose)
1384	δ(C(2)–H(2)) (C(2)–H(2)OH) (cellulose)
1374	δ(C(2)–H(2)) (cellulose C(2)–H(2)OH), or δ(C(2)–H(2)OC=O) (ester)
1356	δ(C(3)–H(3)) (cellulose)
1127	v(C(2)–O(2)) (cellulose) or v(C(2)–O(2)C=O) (ester)
1061	v(C(6)–O(6)) (cellulose) or v(C(6)–O(6)C=O) (ester)

Note: O(2)–H(2) is the generally accepted hydroxyl site on the glucose residues of cellulose, and C(2)–H(2) is the C–H group connected with the corresponding O(2)–H(2) group. Other groups indicate the similar meanings.

Table S2. The sign of cross peaks between 3660 and 3050 cm^{-1} in 2Dcos maps and their changing order.

Cross peaks	Synchronous	Asynchronous	Changing order
(3574 cm^{-1}, 3441 cm^{-1})	+	+	3574 cm^{-1} → 3441 cm^{-1}
(3574 cm^{-1}, 3410 cm^{-1})	+	+	3574 cm^{-1} → 3410 cm^{-1}
(3574 cm^{-1}, 3334 cm^{-1})	+	–	3334 cm^{-1} → 3574 cm^{-1}
(3574 cm^{-1}, 3220 cm^{-1})	+	–	3220 cm^{-1} → 3574 cm^{-1}
(3441 cm^{-1}, 3410 cm^{-1})	+	–	3410 cm^{-1} → 3441 cm^{-1}
(3441 cm^{-1}, 3334 cm^{-1})	+	–	3334 cm^{-1} → 3441 cm^{-1}
(3441 cm^{-1}, 3220 cm^{-1})	+	–	3220 cm^{-1} → 3441 cm^{-1}
(3410 cm^{-1}, 3334 cm^{-1})	+	–	3344 cm^{-1} → 3410 cm^{-1}
(3410 cm^{-1}, 3220 cm^{-1})	+	–	3220 cm^{-1} → 3410 cm^{-1}
(3334 cm^{-1}, 3220 cm^{-1})	+	+	3340 cm^{-1} → 3220 cm^{-1}

Note: In the FTIR spectrum, the related peaks shifted from low wavenumbers to high wavenumbers with the temperature increasing. And the same band shows different wavenumbers in the synchronous and asynchronous maps due to the different resolution levels. The absorbance peak of a functional group can refer to that in the FTIR spectrum when conduct 2Dcos analysis.

Table S3. The sign of cross peaks between 1812 and 1591 cm^{-1} in 2Dcos maps and their changing order.

Cross peaks	Synchronous	Asynchronous	Changing order
(1793 cm^{-1}, 1774 cm^{-1})	+	–	1774 cm^{-1} → 1793 cm^{-1}
(1793 cm^{-1}, 1727 cm^{-1})	–	+	1727 cm^{-1} → 1793 cm^{-1}
(1793 cm^{-1}, 1701 cm^{-1})	+	–	1701 cm^{-1} → 1793 cm^{-1}
(1793 cm^{-1}, 1697 cm^{-1})	+	–	1697 cm^{-1} → 1793 cm^{-1}
(1774 cm^{-1}, 1727 cm^{-1})	+	+	1774 cm^{-1} → 1727 cm^{-1}
(1774 cm^{-1}, 1701 cm^{-1})	+	–	1701 cm^{-1} → 1774 cm^{-1}
(1774 cm^{-1}, 1697 cm^{-1})	+	–	1697 cm^{-1} → 1774 cm^{-1}
(1743 cm^{-1}, 1727 cm^{-1})	+	+	1743 cm^{-1} → 1727 cm^{-1}
(1743 cm^{-1}, 1697 cm^{-1})	–	–	1743 cm^{-1} → 1697 cm^{-1}
(1743 cm^{-1}, 1678 cm^{-1})	–	–	1743 cm^{-1} → 1678 cm^{-1}
(1743 cm^{-1}, 1678 cm^{-1})	–	+	1678 cm^{-1} → 1743 cm^{-1}
(1727 cm^{-1}, 1708 cm^{-1})	+	+	1727 cm^{-1} → 1708 cm^{-1}
(1727 cm^{-1}, 1678 cm^{-1})	–	+	1678 cm^{-1} → 1727 cm^{-1}
(1727 cm^{-1}, 1647 cm^{-1})	–	+	1647 cm^{-1} → 1727 cm^{-1}
(1697 cm^{-1}, 1678 cm^{-1})	+	–	1678 cm^{-1} → 1697 cm^{-1}
(1697 cm^{-1}, 1647 cm^{-1})	+	–	1647 cm^{-1} → 1697 cm^{-1}

References

(1) Guo, Y.; Wu, P. Investigation of the hydrogen-bond structure of cellulose diacetate by two-dimensional infrared correlation spectroscopy. *Carbohydr. Polym.* **2008**, *74*, 509–513.

(2) Hou, L.; Wu, P. Two-dimensional correlation infrared spectroscopy of heat-induced esterification of cellulose with 1,2,3,4-butanetetracarboxylic acid in the presence of sodium hypophosphite. *Cellulose* **2019**, *26*, 2759–2769.

(3) Oh, S. Y.; Yoo, D. I.; Shin,Y.; Kim, H. C.; Kim, H. Y.; Chuang, Y. S.; Park, W. H.; Youk, J. H. Crystalline structure analysis of cellulose treated with sodium hydroxide and carbon dioxide by means of X-ray diffraction and FTIR spectroscopy. *Carbohydr. Res.* **2005**, *340*, 2376–2391.

(4) Watanabe, A.; Morita, S.; Ozaki, Y. Study on temperature-dependent changes in hydrogen bonds in cellulose Iβ by infrared spectroscopy with perturbation-correlation moving-window two-dimensional correlation spectroscopy. *Biomacromolecules* **2006**, *7*, 3164–3170.

(5) Watanabe, A.; Morita, S.; Ozaki, Y. Temperature-dependent changes in hydrogen bonds in cellulose Iα studied by infrared spectroscopy in combination with perturbation-correlation moving-window two-dimensional correlation spectroscopy: Comparison with cellulose Iβ. *Biomacromolecules* **2007**, *8*, 2969–2975.